Am J Cancer Res 2026;16(7):2985-2996
www.ajcr.us /ISSN:2156-6976/ajcr0173351

Original Article

SPP1 promotes the metastasis of liver cancer cells through modulation of the MT1L/vimentin axis

Jen Yu[1,2*], Pei-Huan Ho[1,2*], Chau-Ting Yeh[2], Ming-Wei Lai[2,3], Yang-Hsiang Lin[2,4]

[1]Department of Gastroenterology and Hepatology, Chang Gung Memorial Hospital, Linkou, Taoyuan, Taiwan; [2]Liver Research Center, Chang Gung Memorial Hospital, Linkou, Taoyuan, Taiwan; [3]Department of Pediatrics, Chang Gung Memorial Hospital, Linkou Branch and Chang Gung University College of Medicine, Taoyuan, Taiwan; [4]Graduate Institute of Biomedical Sciences, College of Medicine, Chang Gung University, Taoyuan, Taiwan. [*]Equal contributors.

Received April 15, 2026; Accepted July 7, 2026; Epub July 15, 2026; Published July 30, 2026

Abstract: Tumor metastasis, a hallmark of cancer progression including hepatocellular carcinoma (HCC), is closely linked to poor prognosis. Therefore, strategies to suppress tumor metastasis remain an unresolved challenge for improving patient care. We identified that the oncogenic gene secreted phosphoprotein 1 (SPP1) is highly expressed in HCC tissues. A pseudogene-derived long non-coding RNA, metallothionein 1L (MT1L), was found to be negatively regulated by SPP1. Clinically, MT1L expression was reduced in HCC specimens, and its higher expression correlated positively with favorable prognosis. Notably, MT1L expression was inversely correlated with SPP1 expression in HCC. Mechanistically, SPP1 suppressed MT1L expression through the integrin signaling pathway. Overexpression of MT1L inhibited cell motility and lipid accumulation by repressing vimentin expression. Furthermore, rescue experiments demonstrated that MT1L was functionally involved in SPP1-mediated effects. Collectively, our findings reveal a novel association among the SPP1/MT1L/integrin/vimentin axis in HCC progression, suggesting that targeting this pathway may represent a potential therapeutic approach for HCC.

Keywords: HCC, SPP1, MT1L, metastasis, vimentin

Introduction

Hepatocellular carcinoma (HCC) is one of the most prevalent forms of liver cancer worldwide [1]. Tumor metastasis represents a major determinant of poor prognosis in HCC patients. The metastatic signaling network is highly complex, driven by both intrinsic and extrinsic mechanisms [2, 3]. Therefore, identifying aberrantly expressed genes that drive HCC progression is essential for developing novel therapeutic strategies targeting metastasis.

Secreted phosphoprotein 1 (SPP1), a secreted integrin-binding glycoprotein, plays a critical role in cancer progression [4]. SPP1 is highly expressed in multiple tumor types, including HCC. Through binding to receptors such as integrins and CD44, SPP1 activates downstream signaling cascades that regulate cell survival, metastasis, and angiogenesis [5]. For example, Ng et al. [6] showed that SPP1 promotes migration, invasion, and metastasis of colorectal cancer cells via Twist activation. In ovarian and breast cancers, SPP1 induces hypoxia-inducible factor-1α (HIF-1α), thereby enhancing metastasis and angiogenesis [7, 8]. In HCC, Wang et al. reported that SPP1 is upregulated in tumor tissues compared with normal tissues, and SPP1 knockdown suppressed cell growth and promoted apoptosis through regulation of miR-181c [9]. Moreover, SPP1 has been shown to interact with miRNAs such as miR-340 and miR-433 to modulate cancer cell behavior [9-11]. Collectively, these findings establish SPP1 as a well-recognized oncogene in cancer progression.

Long non-coding RNAs (lncRNAs) function as master regulators of cancer, orchestrating proliferation, metastasis, metabolic reprogramming, and angiogenesis [12]. Among them, pseudogene-derived lncRNAs have emerged as an important subclass implicated in tumor de-

https://doi.org/10.62347/LALC6308

velopment. For instance, protein disulfide isomerase family A member 3 pseudogene 1 (PDIA3P1) is upregulated in HCC and promotes cell growth, migration, and invasion by regulating the p53 signaling pathway [13]. Similarly, ubiquitin-conjugating enzyme E2C pseudogene 3 (UBE2CP3) is overexpressed in HCC and facilitates migration and invasion through the induction of epithelial-mesenchymal transition (EMT)-related genes such as Snail and N-cadherin [14].

Metallothioneins (MTs) are Golgi-localized proteins that bind heavy metals and regulate oxidative stress and metal homeostasis [15-17]. Metallothionein 1L (MT1L) is a pseudogene (NR_001447.2) expressed in various tissues [18]. Recent evidence suggests that elevated MT1L expression correlates with tumor immune infiltration and poor prognosis in bladder cancer [19]. These findings underscore the critical roles of pseudogene-derived lncRNAs in regulating cancer progression. However, the interplay between SPP1 and MT1L in HCC progression remains largely unexplored.

In this study, we demonstrated that SPP1 is highly expressed in HCC tissues and is associated with poor survival. Transcriptome profiling and validation experiments revealed that SPP1 represses MT1L expression in hepatoma cell lines. Functionally, MT1L overexpression suppressed cell proliferation, reduced intracellular iron levels, and inhibited motility. Mechanistically, the SPP1/MT1L axis regulated vimentin expression through integrin-mediated signaling. Our findings identify a novel association between SPP1, MT1L, vimentin, and integrin signaling in HCC, suggesting that targeting this pathway may provide an alternative therapeutic approach for HCC patients.

Materials and methods

Cell lines and reagents

Liver cancer cells, such as HepG2 (RRID: CVCL_0027), Huh7 (RRID: CVCL_0336), Hep3B (RRID: CVCL_0326) and Mahlavu cell lines (CVL_CL-0405), were used in this study. All cells were maintained in Dulbecco's Modified Eagle's Medium (DMEM; Gibco, NY, USA) supplemented with 10% fetal bovine serum (FBS; Gibco), and a combination of 100 μg/mL streptomycin sulfate plus 100 IU/mL penicillin G. The absence of mycoplasma contamination was confirmed using the TOOLS mycoplasma detection kit (BIOTOOLS, New Taipei City, Taiwan; TTB-GBC8).

RNA extraction and quantitative real-time PCR (qRT-PCR)

RNA from cells was purified by TRIzol reagent (Life Technologies). Reverse transcriptase (Life Technologies) converted the RNA to cDNA. In a total volume of 15 μl, the reaction mixture consisted of the target forward and reverse primers, plus 1× SYBR Green Master Mix (Applied Biosystems, Carlsbad, CA) according to the manufacturer's protocol. The amplification parameters were as follows: initial denaturation at 95°C for 10 min and then 40 cycles of 95°C for 15 sec, and annealing at 60°C for 1 min. The following primers were applied: MT1L forward: 5'-GCCTCTCCCGTCATTTCTTG-3'; reverse: 5'-AGGTTCATTTGCACTCTTTGCA-3', Vimentin forward: 5'-GAGAACTTTGCCGTTGAAGC-3'; reverse: 5'-GCTTCCTGTAGGTGGCAATC-3', 18S rRNA forward: 5'-CGAGCCGCCTGGATACC-3'; reverse: 5'-CCTCAGTTCCGAAAACCAACAA-3', GAPDH forward: 5'-AATCCCATCACCATCTTCCA-3'; reverse: 5'-TGGACTCCACGACGTACTCA-3'.

Microarray profiling analysis

RNA integrity from control (sh-luc) and SPP1-depleted cell lines (shSPP1#1 and shSPP1#2) was assessed using the Agilent 2100 Bioanalyzer. Microarray profiling was conducted with the Affymetrix GeneChip Clariom D array (Genomic Medicine Core Laboratory, Chang Gung Memorial Hospital) to explore differentially expressed genes in SPP1-depleted cell lines. SPP1-regulated dysregulated genes were subjected to pathway analysis.

Establishment of SPP1 and MT1L stable cell lines

The coding sequences of SPP1 and MT1L were amplified by PCR and cloned into the pcDNA3 expression vector. The inserted sequences were verified by Sanger sequencing. Short hairpin RNAs (shRNAs) targeting the SPP1 gene (TRCN0000004874 and TRCN0000004875) were obtained from the National RNAi Core Facility (Institute of Molecular Biology, Academia Sinica, Taiwan). In addition, an shRNA tar-

geting MT1L (shMT1L) was designed according to the guidelines of the TRC shRNA design algorithm (RNAi Core Facility, Taiwan) and cloned into the pLKO.1 vector. The shRNA sequences targeting MT1L were as follows: MT1L shRNA-F: 5'-CCGGGTCATTTCTTGGCTCGAAATGCTCGAGCATTTCGAGCCAAGAAATGACTTTTT-3', MT1L shRNA-R: 5'-AATTAAAAAGTCATTTCTTGGCTCGAAATGCTCGAGCATTTCGAGCCAAGAAATGAC-3'. Stable cell lines were maintained in DMEM supplemented with 10% FBS and selected with neomycin and puromycin, respectively. The efficiency of overexpression and knockdown was confirmed by qRT-PCR and western blot analyses.

Western blot analysis

Western blotting was performed as previously described [20]. The following primary antibodies were used: SPP1 (Abcam, ab8448), Vimentin (Abclonal, A11952), and GAPDH (Sigma, G8795). Protein signals were visualized on X-ray film, and intensities of signals were quantified and analyzed by Image Gauge software, normalized to GAPDH.

Cell growth assay

Cell growth was determined using the Alamar Blue cell viability reagent (Invitrogen, DAL1100). Proliferation rates were normalized to the values recorded on day 1.

Transwell assay

Cell migration (non-Matrigel-coated inserts) and invasion (Matrigel-coated inserts) were assessed using Transwell chambers (Becton-Dickinson, Franklin Lakes, NJ, USA). After 24 h of incubation, cells were fixed and stained with crystal violet. Migratory and invasive cells were quantified using ImageJ software.

Iron detection

Intracellular iron levels in MT1L-stable cell lines were measured with the Iron Assay Kit (Abcam, ab83366) and compared with control cells.

BODIPY lipid staining

Intracellular fatty acids in MT1L-stable cell lines were detected by BODIPY staining. Control and MT1L-overexpressing cells were seeded in six-well plates. After 48 h, cells were washed three times with PBS, incubated with 2 μM BODIPY for 20 min at 37°C, and counterstained with Hoechst 33342. Fluorescence signals were imaged and quantified with ImageJ software.

Animal model

To evaluate the metastasis of control and MT1L-overexpressing cell lines, tumor cells (2×10^6 cells) were injected into severe combined immunodeficiency (SCID) mice by tail vein injection. One month after injection, mice were sacrificed and collected the lung tissue. The tumor foci in the lung tissues were monitored by hematoxylin and eosin (H&E) staining. The protocol of animal experiments was followed the guidelines of the United States National Institutes of Health and Chang Gang Institutional Animal Care and Use Committee Guide for the Care and Use of Laboratory Animals (IACUC: CGU111-103).

Statistical analysis

All experiments were conducted three times, and data are given as means ± SD. Statistical analyses were carried out using the IBM SPSS software (version 20; SPSS Inc., Chicago, IL, USA). For comparisons between two groups, we used the t-test of Student's or the Mann-Whitney U tests while for comparisons among multiple groups, one-way ANOVA followed by Tukey post-hoc tests were used. The Kaplan-Meier method was employed to determine differences between groups in survival outcomes using cumulative hazard rates, and the log-rank test was used for comparison. Differences were considered significant if $P < 0.05$.

Results

SPP1 is clinically relevant in HCC progression

To identify master regulators involved in HCC progression, three publicly available datasets (GSE14520, GSE14323, and GSE164760) were analyzed [21-23]. Based on the criteria (T/N ratio > 2 or T/N ratio < 0.5), two potential candidate genes, aldo-keto reductase family 1 member B10 (AKR1B10) and SPP1, were identified (**Figure 1A**). Both AKR1B10 and SPP1 were significantly upregulated in HCC tissues (**Figure 1B**, **1C**). Kaplan-Meier method with the log-rank test was used for survival analysis. No significant differences were observed between

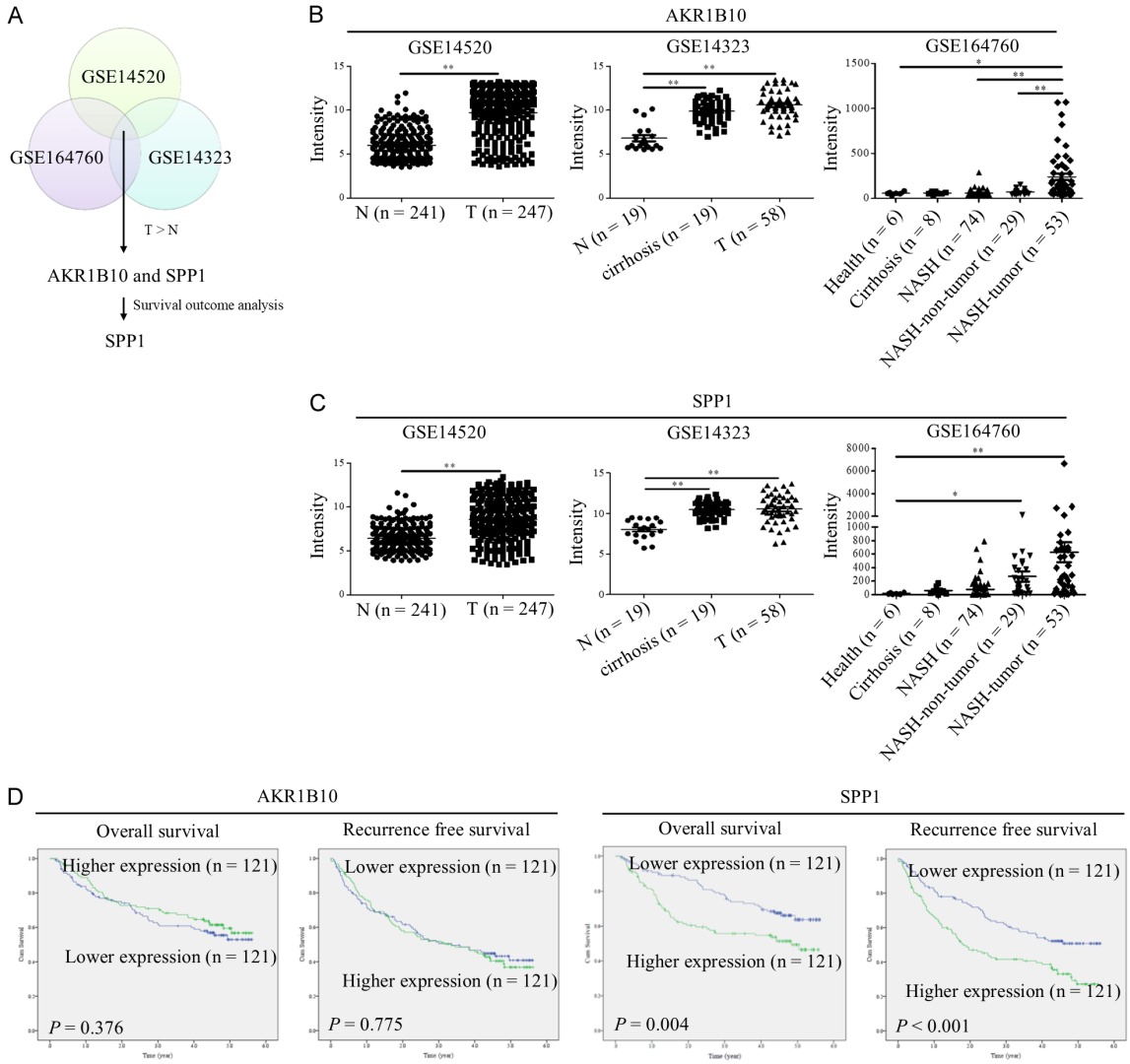

Figure 1. High SPP1 expression is significantly associated with poor survival outcomes. (A) Venn diagram showing differentially expressed genes identified from three publicly available datasets (GSE14520, GSE14323, and GSE164760). (B, C) Expression levels of AKR1B10 (B) and SPP1 (C) across the three datasets. (D) Kaplan-Meier analysis of overall survival and recurrence-free survival according to SPP1 expression in GSE14520. The median expression level of SPP1 was used as the cutoff. Survival differences were assessed using the log-rank test.

AKR1B10-high and AKR1B10-low groups (**Figure 1D**). In contrast, high expression of SPP1 was significantly associated with poor survival outcomes, including overall survival and recurrence-free survival (**Figure 1D**). Moreover, SPP1 expression positively correlated with pathological stage and a predicted metastatic risk signature (**Table 1**). Accordingly, SPP1 was selected for further investigation.

Ectopic expression of SPP1 enhances cell motility in hepatoma cell lines

To validate the bioinformatics findings, SPP1 expression was examined by qRT-PCR in a validation cohort. Consistently, SPP1 was highly expressed in HCC compared to adjacent normal tissues (**Figure 2A**, left panel). Elevated SPP1 expression was associated with shorter recurrence-free survival in HCC patients (**Figure 2A**, right panel). We next explored SPP1-related pathways using GSE14520. Genes correlated with SPP1 were subjected to GSEA analysis, which revealed positive correlations with the hallmarks of G2M checkpoint, EMT, mTORC1 signaling, and hypoxia (**Figure 2B**). To elucidate its functional role, stable SPP1-overexpressing Huh7 cell lines and stable SPP1-knockdown (shSPP1#1 and shSPP1#2) HepG2 and Mahlavu cell lines were established according to their

Table 1. Clinicopathological correlations of SPP1 in HCC specimens (GSE14520)

Parameters	n = 242	SPP1 Mean[a] ± SE	*p*[b]
Age (years)			
< 65	212	8.573 ± 0.1725	0.8815
≥ 65	30	8.511 ± 0.4467	
Gender			
Male	211	8.720 ± 0.1742	0.0092
Female	31	7.515 ± 0.3621	
Age			0.8815
< 65 year	212	8.573 ± 0.1725	
≥ 65 year	30	8.511 ± 0.4467	
Cirrhosis			
No	19	7.571 ± 0.5798	0.0686
Yes	223	8.650 ± 0.1664	
AFP			
Low	128	8.390 ± 0.2358	0.2622
High	110	8.762 ± 0.2146	
Tumor size			
< 5 cm	153	8.361 ± 0.2027	0.0775
≥ 5 cm	88	8.916 ± 0.2608	
Pathological stage			
I	96	7.904 ± 0.2616	0.0020
II	78	8.664 ± 0.2599	
III	51	9.376 ± 0.3413	
Predicted risk Metastasis Signature			
Low	121	9.058 ± 0.0495	0.0006
High	121	9.334 ± 0.0617	

a: Mean of target gene expression in dataset GSE14520; b: Mann-Whitney U test (for two groups) or Kruskal Wallis test (for > two groups).

endogenous SPP1 levels (**Figure 2C**, **2D**). SPP1 knockdown significantly reduced cell migration compared with vector controls (**Figure 2E**, left panel), whereas overexpression promoted migration (**Figure 2E**, right panel). In addition, SPP1 silencing markedly reduced invasive capacity (**Figure 2F**). These findings suggest that SPP1 acts as a master regulator orchestrating oncogenic phenotypes.

MT1L is downregulated by SPP1

To further investigate how SPP1 mediates these phenotypes via lncRNAs, we performed expression profiling in SPP1-depleted HepG2 cells, which revealed several candidate lncRNAs (**Figure 3A**). Pathway analysis indicated an association with the NAFLD phenotype (highlighted in red, **Figure 3B**). qRT-PCR validation confirmed that MT1L expression was significantly upregulated in SPP1-depleted HepG2 cells, while SPP1 overexpression suppressed MT1L expression (**Figure 3C**), consistent with the profiling results. Clinically, MT1L was significantly lower expressed in HCC tissues compared with adjacent normal tissues in both TCGA and our validation cohort (**Figure 3D**). Higher MT1L expression correlated with better clinical outcomes (**Figure 3E**), suggesting a tumor-suppressive role. Importantly, MT1L expression was inversely correlated with SPP1 expression in the validation cohort (**Figure 3F**).

MT1L suppresses cell growth, migration, invasion, and iron levels in hepatoma cells

To investigate the functional role of MT1L, stable MT1L-overexpressing HepG2 and Mahlavu cell lines (MT1L-1 and MT1L-2) were established (**Figure 4A**). Oleic acid (OA) treatment markedly induced lipid accumulation in control cells, whereas this effect was significantly attenuated in MT1L-overexpressing cells (**Figure 4B**), suggesting that MT1L may play a role in regulating OA-induced lipid accumulation. Consistent with this finding, ectopic expression of MT1L also reduced intracellular iron levels (**Figure 4C**). Furthermore, MT1L overexpression significantly suppressed cell growth, migration, and invasion compared with control cells (**Figure 4D**, **4E**). These results indicate that MT1L functions as a tumor suppressor in HCC. To further confirm that the *in vitro* phenotypes of MT1L were similar to those observed *in vivo*, the metastatic ability of MT1L was examined in SCID mice. The results demonstrated that ectopic expression of MT1*L remarkably supp*ressed tumor metastasis compared with the control group (**Figure 4F**). To further determine whether MT1L modulates SPP1-mediated cell motility, Transwell migration assays were performed in cells

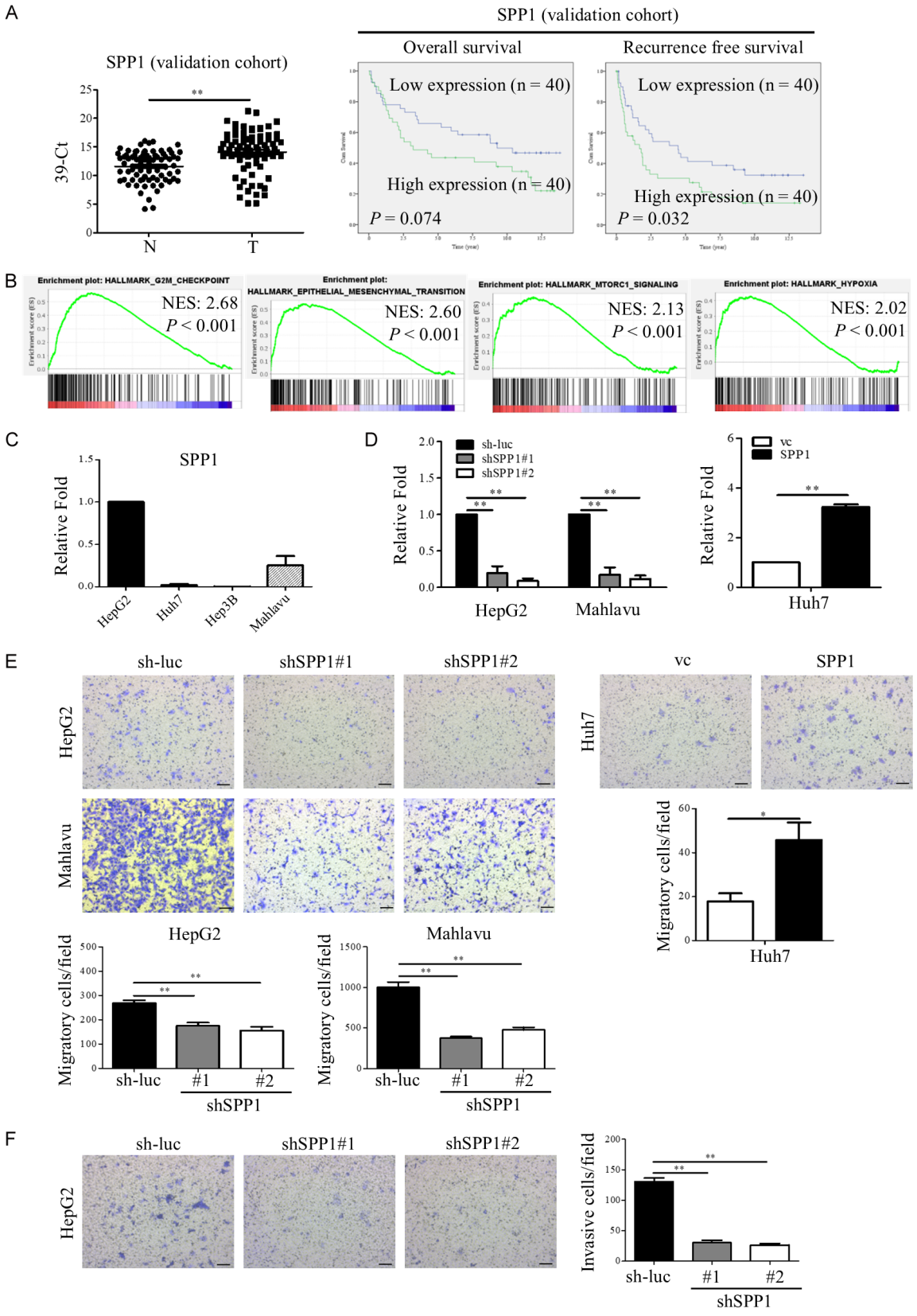

Figure 2. Overexpression of SPP1 enhances cell motility in hepatoma cell lines. A. In the validation cohort, SPP1 was significantly upregulated in HCC tissues compared with adjacent normal tissues. Kaplan-Meier analysis of overall survival and recurrence-free survival was performed according to SPP1 expression levels in the validation cohort. The median expression level of SPP1 was used as the cutoff, and survival differences were assessed using the log-

rank test. B. SPP1-associated pathways in GSE14520 were analyzed using GSEA software. C. Basal SPP1 mRNA levels in parental HCC cell lines were determined by qRT-PCR, with GAPDH used as the internal control. D. SPP1 expression in stable SPP1 knockdown and overexpression cell lines was measured by qRT-PCR, with GAPDH as the internal control. E. Cell migration in stable SPP1 knockdown and overexpression cell lines was assessed using the Transwell migration assay. Migratory cells were stained with crystal violet and quantified using ImageJ software. Scale bar: 100 μm. F. Cell invasion was examined in SPP1-depleted HepG2 cell lines. Invasive cells were stained with crystal violet and quantified using ImageJ software. Scale bar: 100 μm.

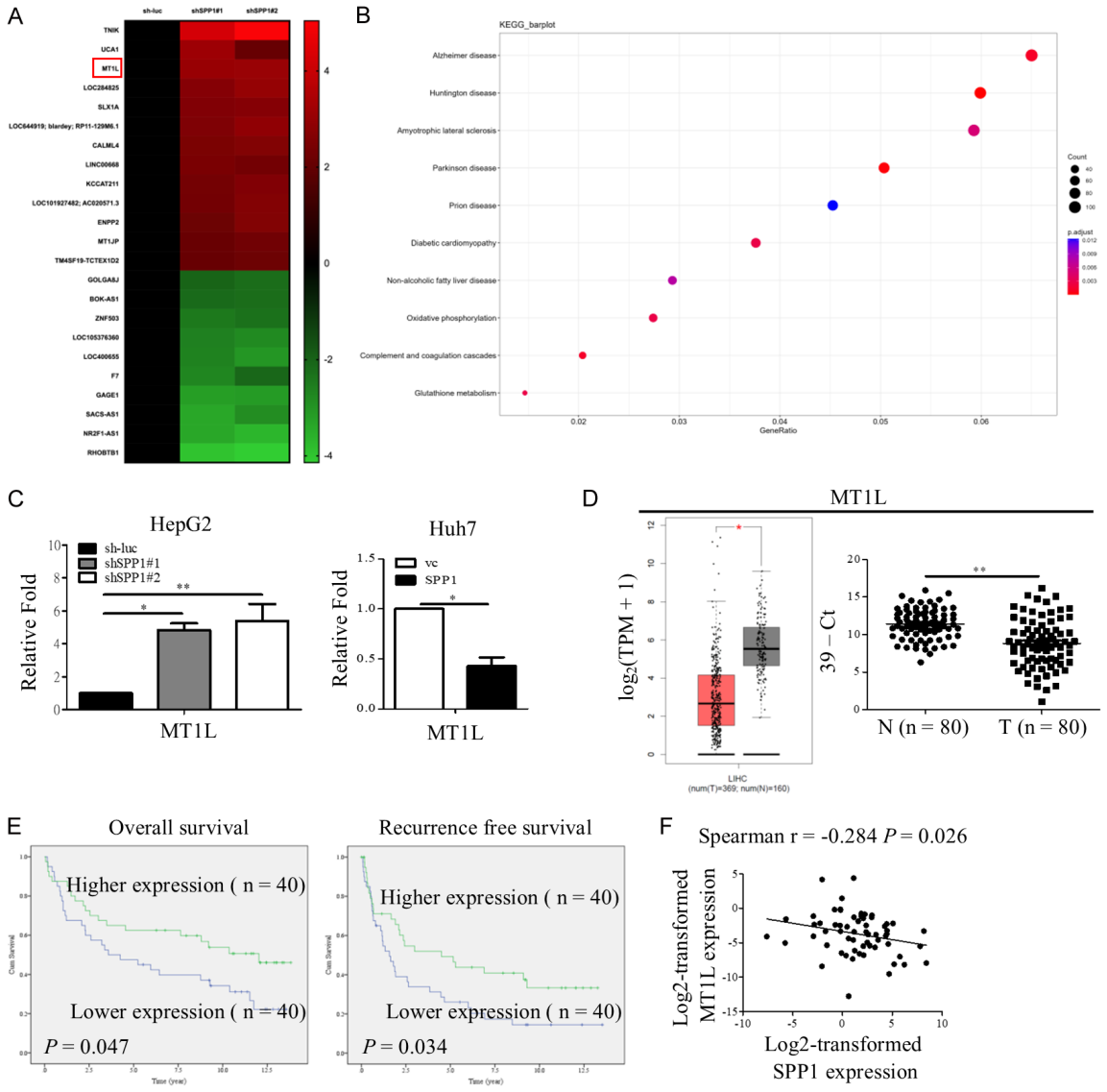

Figure 3. MT1L is downregulated in HCC tissues and correlated with survival outcomes. A. Heat map showing differentially expressed lncRNAs regulated by SPP1. B. KEGG pathway analysis of SPP1-mediated signaling pathways. C. MT1L expression levels in stable SPP1 knockdown and overexpression cell lines were determined by qRT-PCR, with 18S rRNA used as the internal control. D. MT1L expression in the TCGA dataset and in the validation cohort was measured by qRT-PCR, with 18S rRNA used as the internal control. E. Kaplan-Meier analysis of overall survival and recurrence-free survival according to MT1L expression in the validation cohort. The median expression level of MT1L was used as the cutoff, and survival differences were assessed using the log-rank test. F. Correlation between SPP1 and MT1L expression in the validation cohort was analyzed using Spearman's correlation coefficient.

with simultaneous overexpression or knockdown of MT1L and SPP1. SPP1 overexpression significantly enhanced cell migration, whereas this promotive effect was partially attenuated

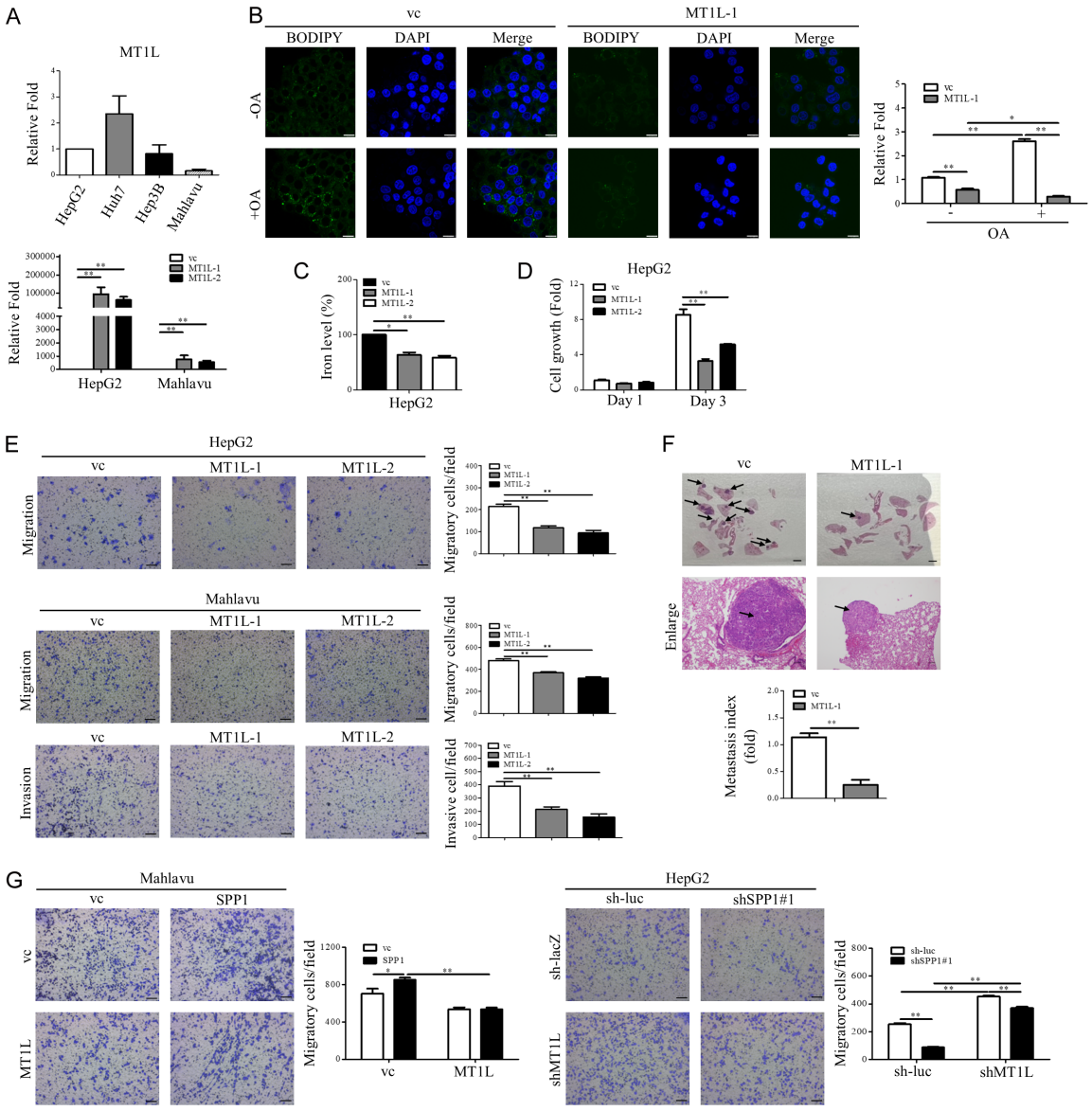

Figure 4. MT1L functions as a tumor-suppressive lncRNA in hepatoma cell lines. A. Expression levels of MT1L in parental hepatoma cells and stable MT1L-overexpressing cell lines determined by qRT-PCR, with 18S rRNA as the internal control. B. Representative BODIPY staining images showing lipid accumulation in control and MT1L-overexpressing Mahlavu cells with or without oleic acid (OA) treatment. Scale bar: 10 μm. C. Intracellular iron levels in control and MT1L-overexpressing HepG2 cells. Relative iron levels were compared with vector control (vc). D. Cell growth curves of HepG2 cells stably overexpressing MT1L measured at days 1 and 3. E. Transwell migration assays of HepG2 and Mahlavu cells (upper panels) and invasion assays of Mahlavu cells (lower panels). Representative images (left) and quantification of migratory and invasive cells (right) are shown. Cells were stained with crystal violet and quantified using ImageJ software. Scale bar: 100 μm. F. Tumor metastasis in the vector control (vc) and MT1L-overexpression group (MT1L) was quantified. The arrowheads indicated tumor foci in the H&E-stained sections. Quantification of relative lipid accumulation is shown (right). Scale bar: 500 μm (upper panels) and 100 μm (lower enlarged panels). G. Left panel: Transwell migration assays of Mahlavu cells with simultaneous overexpression of SPP1 and MT1L. Right panel: Transwell migration assays of HepG2 cells with simultaneous knockdown of SPP1 and MT1L. Representative images and quantification of migratory cells are shown. Cells were stained with crystal violet and quantified using ImageJ software. Scale bar: 100 μm. Data are presented as mean ± SD; *P < 0.05, **P < 0.01.

by the concomitant overexpression of MT1L (**Figure 4G**, left panel). Conversely, SPP1 knockdown markedly suppressed cell migration, and this inhibitory phenotype was partially rescued by the simultaneous knockdown of MT1L (**Figure 4G**, right panel). Together, these find-

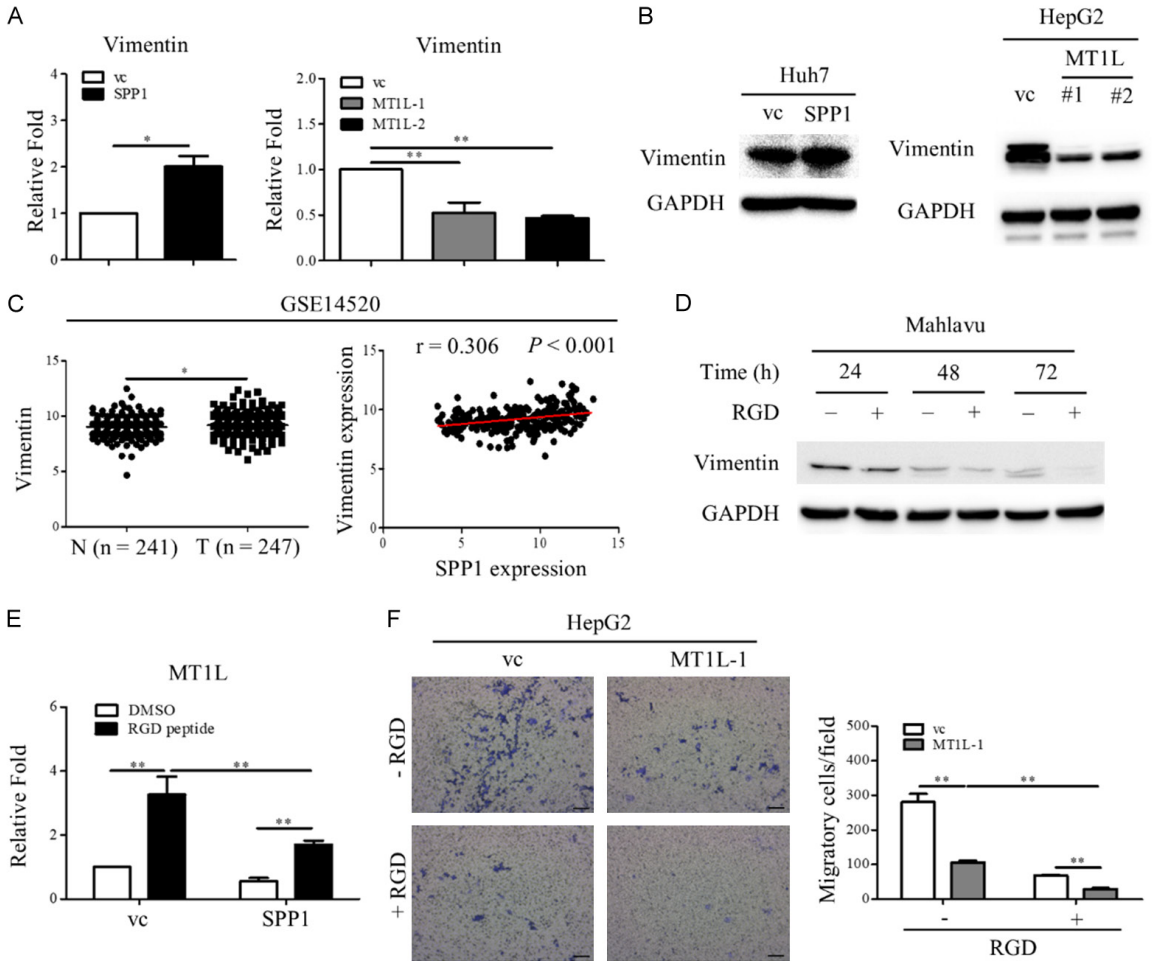

Figure 5. The SPP1/MT1L axis regulates vimentin expression via integrin signaling. A. Vimentin mRNA expression in control, SPP1-overexpressing, and MT1L-overexpressing hepatoma cells determined by qRT-PCR, with GAPDH as the internal control. B. Western blot analysis of vimentin protein levels in control, SPP1-overexpressing, and MT1L-overexpressing cell lines. GAPDH served as a loading control. C. Vimentin expression in HCC tissues from the GSE14520 dataset (left) and correlation between SPP1 and vimentin expression (right). D. Western blot analysis of vimentin expression in Mahlavu cells treated with or without RGD peptide for 24, 48, and 72 h. E. MT1L expression in control and SPP1-overexpressing cells treated with DMSO or RGD peptide, determined by qRT-PCR. 18S rRNA was used as the internal control. F. Transwell migration assays of control (vc) and MT1L-overexpressing cells treated with or without RGD peptide. Representative images (left) and quantification of migratory cells (right) are shown. Cells were stained with crystal violet and quantified using ImageJ software. Scale bar: 100 μm. Data are presented as mean ± SD; *P < 0.05, **P < 0.01.

ings indicate that MT1L antagonizes SPP1-mediated oncogenic functions.

Vimentin is regulated by the SPP1/MT1L axis

Intermediate filaments (IFs) are key regulators of cellular functions, including proliferation, motility, and drug resistance [24]. To determine whether vimentin, a major IF protein, is regulated by the SPP1/MT1L axis, its expression was examined in liver cancer cell lines. qRT-PCR and western blot analyses revealed that SPP1 overexpression enhanced vimentin levels, whereas MT1L overexpression suppressed vimentin expression (**Figure 5A**, **5B**). Clinically, vimentin was upregulated in HCC tissues (GSE14520) (**Figure 5C**, left panel), and SPP1 expression positively correlated with vimentin (**Figure 5C**, right panel). SPP1 contains an arginine-glycine-aspartic acid (RGD) domain that binds integrins [25], thereby activating integrin-mediated signaling. To test whether vimentin regulation depends on the RGD domain, Mahlavu cells were treated with RGD peptide.

Western blotting showed that RGD peptide treatment reduced vimentin expression in a time-dependent manner (**Figure 5D**), while simultaneously promoting MT1L expression in both control and SPP1-overexpressing cells (**Figure 5E**). Functionally, MT1L overexpression suppressed migration, and this effect was further enhanced by RGD peptide treatment (**Figure 5F**). Collectively, these findings indicate that SPP1/MT1L-mediated regulation of vimentin occurs through an integrin-dependent pathway.

Discussion

Multiple studies, along with our findings, have uncovered that SPP1 functions as an oncogenic factor in HCC progression [26]. Ectopic expression of SPP1 enhanced cell growth and motility in hepatoma cell lines. However, the underlying mechanisms by which SPP1 promotes cancer progression through pseudogene-derived lncRNAs remain unclear. In this study, we first identified that a pseudogene-derived lncRNA, MT1L, was downregulated by SPP1, as shown by microarray profiling and validated by qRT-PCR. Furthermore, treatment with an RGD peptide, an integrin receptor inhibitor, induced MT1L expression. Taken together, these findings indicate that MT1L expression is regulated by the SPP1/integrin pathway.

To date, the information of functional role of MT1L in cancer progression has been limited. Ding et al. demonstrated that MT1L expression was downregulated in bladder cancer tissues [19]. Another study showed that MT1L expression was decreased in prostate adenocarcinoma cell lines compared to RWPE-1, a normal prostate cell line [27]. Functionally, overexpression of MT1L in PC-3 cells reduced cell growth and migration while promoting apoptosis. In our study, overexpression of MT1L suppressed cell growth, intracellular iron levels, migration, and invasion in liver cancer cell lines. Notably, vimentin expression was repressed upon MT1L overexpression. Rescue experiments further supported that MT1L participates in SPP1/integrin pathway-mediated regulation of vimentin expression. Clinically, MT1L was significantly downregulated in HCC tissues, while elevated MT1L expression was associated with better prognosis. Moreover, MT1L expression levels were negatively correlated with SPP1 expression in HCC tissues. Together, these findings highlight the significance of the SPP1/MT1L axis in HCC progression, suggesting that MT1L plays an important tumor-suppressive role.

A previous study reported that a lncRNA named vimentin-associated lncRNA (VAL) was induced by AKT/STAT3 signaling, leading to enhance tumor invasion, metastasis, and anoikis resistance in lung adenocarcinoma [28]. Mechanistically, VAL enhanced oncogenic effects by directly interacting with vimentin and blocking Trim16-mediated polyubiquitination and degradation of vimentin. Zhang et al. demonstrated that elevated expression of circular RNA KEAP1 (circKEAP1) reduced osteosarcoma cell proliferation, stemness, and motility [29]. Interestingly, circKEAP1 encoded a truncated protein, KEAP1-259aa, which interacted with vimentin and promoted its proteasomal degradation. These findings suggest that lncRNAs and circRNAs regulate vimentin primarily at the post-translational level. By contrast, our results revealed that vimentin mRNA expression is regulated by the SPP1/MT1L/integrin pathway, indicating a transcriptional mechanism. Thus, regulation of vimentin may occur through distinct mechanisms depending on the model system.

In conclusion, we identified MT1L as a negative regulator downstream of the SPP1/integrin pathway. MT1L attenuated SPP1-enhanced cell growth and motility, with vimentin serving as a key downstream effector of the SPP1/MT1L axis (**Figure 6**). Collectively, our study establishes a novel regulatory association among SPP1, MT1L, vimentin, and the RGD peptide in HCC progression, which may provide a potential therapeutic strategy for treating HCC.

Acknowledgements

We would like to thank Taiwan Liver Cancer Network (TLCN) for providing the hepatoma tissue samples and related clinical data (all are anonymous) for our research work. We also thank the Genomic Medicine Core Laboratory, Chang Gung Memorial Hospital, Linkou, Taiwan, for performing gene expression profiling and providing data analysis support. This work was supported by grants from Chang Gung Memorial Hospital, Taoyuan, Taiwan (CMRPG-3M2181-2183 to YHL).

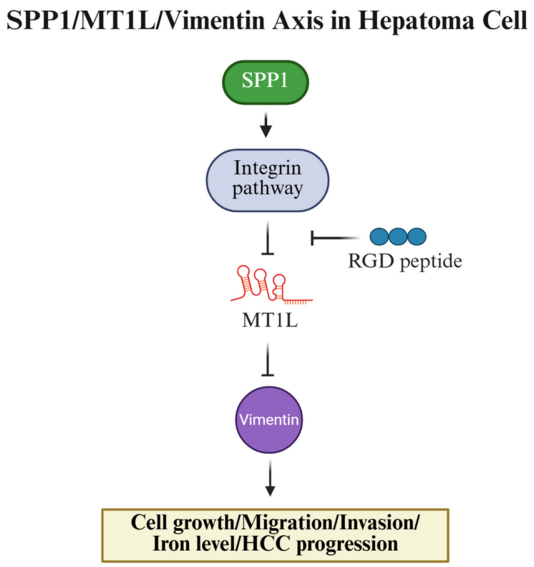

Figure 6. A model of the SPP1/integrin/MTL1/vimentin cascade in HCC progression. This schematic illustrates the SPP1/MT1L/Vimentin signaling axis in hepatoma cells. SPP1 activates the integrin pathway, which subsequently regulates MT1L expression. MT1L then modulates vimentin, leading to enhanced cell growth, migration, invasion, iron regulation, and HCC progression. Notably, the integrin pathway can be inhibited by RGD peptides, indicating a potential therapeutic intervention point. This figure was created using BioRender.com.

Disclosure of conflict of interest

None.

Abbreviations

HCC, hepatocellular carcinoma; SPP1, secreted phosphoprotein 1; HIF-1α, hypoxia-inducible factor-1α; lncRNA, long non-coding RNA; PDIA3P1, protein disulfide isomerase family A member 3 pseudogene 1; UBE2CP3, ubiquitin-conjugating enzyme E2C pseudogene 3; EMT, epithelial-mesenchymal transition; MT, metallothionein; MT1L, metallothionein 1L; AKR1B10, aldo-keto reductase family 1 member B10; SCID, severe combined immunodeficiency; H&E staining, hematoxylin and eosin staining; OA, oleic acid; IF, intermediate filament; VAL, vimentin-associated lncRNA; circKEAP1, circular RNA KEAP1.

Address correspondence to: Dr. Yang-Hsiang Lin, Liver Research Center, Chang Gung Memorial Hospital, No. 15, Wenhua 1st Road, Guishan District, Linkou, Taoyuan 333, Taiwan. Tel: +886-3-3281200 Ext. 7717; Fax: +886-3-3281200 Ext. 7717; E-mail: yhlin0621@cgmh.org.tw

References

[1] Sanyal AJ, Yoon SK and Lencioni R. The etiology of hepatocellular carcinoma and consequences for treatment. Oncologist 2010; 15 Suppl 4: 14-22.

[2] Uchino K, Tateishi R, Shiina S, Kanda M, Masuzaki R, Kondo Y, Goto T, Omata M, Yoshida H and Koike K. Hepatocellular carcinoma with extrahepatic metastasis: clinical features and prognostic factors. Cancer 2011; 117: 4475-4483.

[3] Huang F, Wang BR and Wang YG. Role of autophagy in tumorigenesis, metastasis, targeted therapy and drug resistance of hepatocellular carcinoma. World J Gastroenterol 2018; 24: 4643-4651.

[4] Wei T, Bi G, Bian Y, Ruan S, Yuan G, Xie H, Zhao M, Shen R, Zhu Y, Wang Q, Yang Y and Zhu D. The significance of secreted phosphoprotein 1 in multiple human cancers. Front Mol Biosci 2020; 7: 565383.

[5] Fnu G, Agrawal P, Kundu GC and Weber GF. Structural constraint of osteopontin facilitates efficient binding to CD44. Biomolecules 2021; 11: 813.

[6] Ng L, Wan TM, Lam CS, Chow AK, Wong SK, Man JH, Li HS, Cheng NS, Pak RC, Cheung AH, Yau TC, Lo OS, Foo DC, Poon JT, Poon RT, Pang RW and Law WL. Post-operative plasma osteopontin predicts distant metastasis in human colorectal cancer. PLoS One 2015; 10: e0126219.

[7] Song G, Cai QF, Mao YB, Ming YL, Bao SD and Ouyang GL. Osteopontin promotes ovarian cancer progression and cell survival and increases HIF-1alpha expression through the PI3-K/Akt pathway. Cancer Sci 2008; 99: 1901-1907.

[8] Raja R, Kale S, Thorat D, Soundararajan G, Lohite K, Mane A, Karnik S and Kundu GC. Hypoxia-driven osteopontin contributes to breast tumor growth through modulation of HIF1alpha-mediated VEGF-dependent angiogenesis. Oncogene 2014; 33: 2053-2064.

[9] Wang J, Hao F, Fei X and Chen Y. SPP1 functions as an enhancer of cell growth in hepatocellular carcinoma targeted by miR-181c. Am J Transl Res 2019; 11: 6924-6937.

[10] Song SZ, Lin S, Liu JN, Zhang MB, Du YT, Zhang DD, Xu WH and Wang HB. Targeting of SPP1 by microRNA-340 inhibits gastric cancer cell epithelial-mesenchymal transition through inhibition of the PI3K/AKT signaling pathway. J Cell Physiol 2019; 234: 18587-18601.

[11] Han Z, Shi F, Chen Y, Dong X, Zhang B and Li M. Relationship between miRNA-433 and SPP1 in the presence of fracture and traumatic brain injury. Exp Ther Med 2021; 22: 928.
[12] Zhang XZ, Liu H and Chen SR. Mechanisms of long non-coding rnas in cancers and their dynamic regulations. Cancers (Basel) 2020; 12: 1245.
[13] Kong Y, Zhang L, Huang Y, He T, Zhang L, Zhao X, Zhou X, Zhou D, Yan Y, Zhou J, Xie H, Zhou L, Zheng S and Wang W. Pseudogene PDIA3P1 promotes cell proliferation, migration and invasion, and suppresses apoptosis in hepatocellular carcinoma by regulating the p53 pathway. Cancer Lett 2017; 407: 76-83.
[14] Cao SW, Huang JL, Chen J, Hu YW, Hu XM, Ren TY, Zheng SH, Lin JD, Tang J, Zheng L and Wang Q. Long non-coding RNA UBE2CP3 promotes tumor metastasis by inducing epithelial-mesenchymal transition in hepatocellular carcinoma. Oncotarget 2017; 8: 65370-65385.
[15] Thirumoorthy N, Shyam Sunder A, Manisenthil Kumar K, Senthil Kumar M, Ganesh G and Chatterjee M. A review of metallothionein isoforms and their role in pathophysiology. World J Surg Oncol 2011; 9: 54.
[16] Arriaga JM, Levy EM, Bravo AI, Bayo SM, Amat M, Aris M, Hannois A, Bruno L, Roberti MP, Loria FS, Pairola A, Huertas E, Mordoh J and Bianchini M. Metallothionein expression in colorectal cancer: relevance of different isoforms for tumor progression and patient survival. Hum Pathol 2012; 43: 197-208.
[17] Ruttkay-Nedecky B, Nejdl L, Gumulec J, Zitka O, Masarik M, Eckschlager T, Stiborova M, Adam V and Kizek R. The role of metallothionein in oxidative stress. Int J Mol Sci 2013; 14: 6044-6066.
[18] Holloway AF, Stennard FA and West AK. Human metallothionein gene MT1L mRNA is present in several human tissues but is unlikely to produce a metallothionein protein. FEBS Lett 1997; 404: 41-44.
[19] Ding Y, Liu N, Chen M, Xu Y, Fang S, Xiang W, Hua X, Chen G, Zhong Y and Yu H. Overexpressed pseudogene MT1L associated with tumor immune infiltrates and indicates a worse prognosis in BLCA. World J Surg Oncol 2021; 19: 133.
[20] Lin YH, Chi HC, Wu MH, Liao CJ, Chen CY, Huang PS, Huang WC, Wang YW, Lin TK, Lai MW, Yeh CT and Lin KH. The novel role of LOC344887 in the enhancement of hepatocellular carcinoma progression via modulation of SHP1-regulated STAT3/HMGA2 signaling axis. Int J Biol Sci 2024; 20: 6281-6296.
[21] Roessler S, Jia HL, Budhu A, Forgues M, Ye QH, Lee JS, Thorgeirsson SS, Sun Z, Tang ZY, Qin LX and Wang XW. A unique metastasis gene signature enables prediction of tumor relapse in early-stage hepatocellular carcinoma patients. Cancer Res 2010; 70: 10202-10212.
[22] Mas VR, Maluf DG, Archer KJ, Yanek K, Kong X, Kulik L, Freise CE, Olthoff KM, Ghobrial RM, McIver P and Fisher R. Genes involved in viral carcinogenesis and tumor initiation in hepatitis C virus-induced hepatocellular carcinoma. Mol Med 2009; 15: 85-94.
[23] Pinyol R, Torrecilla S, Wang H, Montironi C, Piqué-Gili M, Torres-Martin M, Wei-Qiang L, Willoughby CE, Ramadori P, Andreu-Oller C, Taik P, Lee YA, Moeini A, Peix J, Faure-Dupuy S, Riedl T, Schuehle S, Oliveira CP, Alves VA, Boffetta P, Lachenmayer A, Roessler S, Minguez B, Schirmacher P, Dufour JF, Thung SN, Reeves HL, Carrilho FJ, Chang C, Uzilov AV, Heikenwalder M, Sanyal A, Friedman SL, Sia D and Llovet JM. Molecular characterisation of hepatocellular carcinoma in patients with non-alcoholic steatohepatitis. J Hepatol 2021; 75: 865-878.
[24] Strouhalova K, Přechová M, Gandalovičová A, Brábek J, Gregor M and Rosel D. Vimentin intermediate filaments as potential target for cancer treatment. Cancers (Basel) 2020; 12: 184.
[25] Tan Y, Zhao L, Yang YG and Liu W. The role of osteopontin in tumor progression through tumor-associated macrophages. Front Oncol 2022; 12: 953283.
[26] Tong W, Wang T, Bai Y, Yang X, Han P, Zhu L, Zhang Y and Shen Z. Spatial transcriptomics reveals tumor-derived SPP1 induces fibroblast chemotaxis and activation in the hepatocellular carcinoma microenvironment. J Transl Med 2024; 22: 840.
[27] Liu L, Li Y, Tang S, Yang B, Zhang Q, Xiao R, Hou X, Liu C and Ma L. Gleason Score-related MT1L as biomarker for prognosis in prostate adenocarcinoma and contribute to tumor progression in vitro. Int J Biol Markers 2023; 38: 114-123.
[28] Tian H, Lian R, Li Y, Liu C, Liang S, Li W, Tao T, Wu X, Ye Y, Yang X, Han J, Chen X, Li J, He Y, Li M, Wu J and Cai J. AKT-induced lncRNA VAL promotes EMT-independent metastasis through diminishing Trim16-dependent Vimentin degradation. Nat Commun 2020; 11: 5127.
[29] Zhang Y, Liu Z, Zhong Z, Ji Y, Guo H, Wang W and Chen C. A tumor suppressor protein encoded by circKEAP1 inhibits osteosarcoma cell stemness and metastasis by promoting vimentin proteasome degradation and activating anti-tumor immunity. J Exp Clin Cancer Res 2024; 43: 52.